Universal Decay Cascade Model for Dynamic Quantum Dot Initialization

Vyacheslavs Kashcheyevs[1,2] and Bernd Kaestner[3]

[1]*Faculty of Computing, University of Latvia, Riga LV-1586, Latvia*
[2]*Faculty of Physics and Mathematics, University of Latvia, Riga LV-1002, Latvia*
[3]*Physikalisch-Technische Bundesanstalt, Bundesallee 100, 38116 Braunschweig, Germany*

Dynamic quantum dots can be formed by time-dependent electrostatic potentials, such as in gate- or surface-acoustic-wave-driven electron pumps. In this work we propose and quantify a scheme to initialize quantum dots with a controllable number of electrons. It is based on a rapid increase of the electron potential energy and simultaneous decoupling from the source lead. The full probability distribution for the final number of captured electrons is obtained by solving a master equation for stochastic cascade of single electron escape events. We derive an explicit fitting formula to extract the sequence of decay rate ratios from the measurements of averaged current in a periodically driven device. This provides a device-specific fingerprint which allows us to compare different architectures, and predict the upper limits of initialization accuracy from low precision measurements.

Single electron charging effects have attracted much interest since the proposal of single electronics [1] and the possibility to fabricate nanoscale structures. In particular, quantum dots (QD) connected to leads have been a standard model system for many years to study single charges in so-called artificial atoms. Dynamic QDs, which are repeatedly formed and manipulated by time-varying confining potentials appear, in particular, in structures proposed to study quantum information [2–7]. One of the issues to be addressed is the decoupling of the QD from the environment and at the same time allowing the fast initialization with a controllable number of electrons. A suitable method has been demonstrated by Kataoka *et al.* [6] which uses pulses of surface acoustic waves (SAWs) to populate or depopulate a QD that is well isolated from electron reservoirs. While this mechanism is not yet fully understood, a more conventional approach [8] is adiabatic decoupling of the QD from the electron reservoir, keeping the voltage on the QD fixed in a Coulomb blockade valley separating the discrete charge states. This strategy is limited by (i) nonadiabatic excitation of the QD [9] due to the necessary finite decoupling rate, and (ii) experimental difficulties in tuning the lead-dot coupling to zero without disturbing the electrostatic potential on the QD, φ.

Here we propose and quantify an alternative scheme to achieve initialization by allowing nonequilibrium relaxation (backtunneling) from a QD being raised energetically above the Fermi level during the decoupling process. This process is known to play a role in several types of nonadiabatic current generation devices [10–14]. We identify scale separation in integrated time-dependent electron escape rates between the subsequent charge states as a precondition for low-dispersion initialization. In our decay-cascade model a voltage parameter V shifts the hierarchy of the decay rates and thereby tunes the target number of

electrons, n_0, and the corresponding error $\langle (n - n_0)^2 \rangle$. The minimal error is then given by the particular QD implementation and fixed, for instance, by QD geometry. We proceed to analyze the results of recent nonadiabatic current generation experiments [15–17] and find them to be promising realizations of the proposed initialization scheme. Based on the decay-cascade model predictions we propose an indirect way to measure the initialization accuracy in these devices by extracting the decay rate hierarchy fingerprint from low precision measurements of their current-voltage characteristics. Finally, possible strategies for accuracy improvement are discussed based on the ways charging energy, temperature and barrier design affect the electron escape rates.

Decay-cascade model.—The initialization process is shown pictorially in Fig. 1(a). The relaxation rate of electrons in the QD, $\Gamma_{RC} = (RC)^{-1}$, is reduced at a characteristic speed $\beta = |\dot{\Gamma}_{RC}/\Gamma_{RC}|$. (Here R and C are the resistance and the capacitance of the QD with respect to its environment, respectively.) Simultaneously, $\varphi(t)$ grows more negative. Ejection of electrons at rate $\Gamma_{ad} = |e\dot{\varphi}/E_c|$ is required for the electron number distribution $P_n(t)$ to stay close to instantaneous equilibrium ($E_c = e^2/C$ is the charging energy and e is the electron charge). Such adiabatic following becomes impossible due to insufficient escape rate at times beyond the nonadiabatic crossover time t_0 defined by $\Gamma_{RC}(t_0) = \Gamma_{ad}$. Crucially for our scheme, if Γ_{ad} can be made much larger than β then excitation from the Fermi sea [9] can be ignored while the QD remains loose enough at $t > t_0$ to "forget" the adiabatic initial condition $P_n(t_0)$ and yield eventual accuracy dictated by the decay-cascade mechanism.

For $t > t_0$ we write down a general kinetic equation

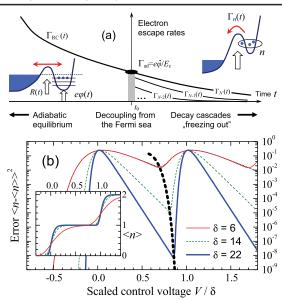$$dP_n(t)/dt = -\Gamma_n(t)P_n(t) + \Gamma_{n+1}(t)P_{n+1}(t), \quad (1)$$

FIG. 1 (color online). (a) Overview of the model. (b) Main results: the variance, $\langle n - \langle n \rangle \rangle^2$, and the average (inset), $\langle n \rangle$, of the number of captured electrons n, for $\alpha_n = 1$, $\delta_1 = 0$ and $\delta_n = \delta$ as functions of control voltage V (in units of δ). All results are calculated using $N = 5$ and Eq. (4), except for the thin dotted line that shows Eq. (10) with $N = 2$. The thick dotted line traces the position and the value of variance as δ is varied.

$$P_n(t_0) = \delta_{n,N}, \qquad \lim_{t \to \infty} \Gamma_n(t) = 0, \qquad (2)$$

where Γ_n is the decay rate of the charge state with n electrons on the QD. The empty dot ($n = 0$) is an absorbing state, $\Gamma_0 \equiv 0$, and the distribution is normalized, $\sum_{n=0}^{\infty} P_n = 1$. N is the initial number of electrons and $\Gamma_N(t_0)$ is identified with Γ_{ad} [see Fig. 1(a)]. The use of Eqs. (1) and (2) to describe QD initialization assumes (i) randomization of the microstate corresponding to a given n on a time scale $\tau \ll \Gamma_n^{-1}$ so that Markov approximation is justified and the transition rates Γ_n are well defined, (ii) no additional loading of electrons into the QD after t_0, and (iii) the sharp initial condition, Eq. (2) (the latter is nonessential). The system of equations (1) is rather general, and has also been used in the context of dynamic QD evolution [13,18] (although not for the initialization stage).

A general iterative solution to Eq. (1) is

$$P_n(t) = \int_{t_0}^{t} e^{-\int_{t'}^{t} \Gamma_n(\tau)d\tau} \Gamma_{n+1}(t') P_{n+1}(t') dt', \qquad (3)$$

for $n < N$ and $P_N(t) = \exp(-\int_{t_0}^{t} \Gamma_N(\tau)d\tau)$ ensures fulfillment of the initial condition (2). Our strategy is, firstly, to identify the general properties of Eq. (3) that result in a well-defined final electron number, and, second, to introduce more specific physical assumptions that connect the model with potential experimental realizations.

Conditions for accurate initialization.—Consider an additional assumption (which can be relaxed later) that time dependence of $\Gamma_n(t)$ is the same for all n, namely,

$\Gamma_n(t)/\Gamma_{n-1}(t) \equiv e^{\delta_n} = \text{const}$. In this case the final ($t \to \infty$) distribution P_n depends only on the dimensionless integrals $X_n \equiv \int_{t_0}^{\infty} \Gamma_n(t)dt$ and is given by

$$P_n(\infty) = \sum_{k=n}^{N} Q_{nk} C_k e^{-X_k}, \qquad (4)$$

$$C_k = - \sum_{m=k+1}^{N} C_m Q_{km}; \qquad C_N = 1, \qquad (5)$$

$$Q_{nk} = \prod_{m=n}^{k-1} \frac{X_{m+1}}{X_m - X_k}; \qquad Q_{nn} = 1. \qquad (6)$$

The solution (4) is rather unilluminating, but can be investigated numerically (see below). For now let us focus on the limit of cascade time-scale separation:

$$\ldots \gg X_{n+1} \gg X_n \gg X_{n-1} \gg \ldots. \qquad (7)$$

In this limit Eq. (6) simplifies to $Q_{k-1,k} = -1$ and $Q_{nk} = 0$ for all $n < k - 1$. This in turn means that $C_n = 1$ for all $0 \le n \le N$. The solution becomes $P_N(\infty) = e^{-X_N}$ and

$$P_n(\infty) = e^{-X_n} - e^{-X_{n+1}} \quad \text{for } 0 \le n < N. \qquad (8)$$

Our model is justified for $\Gamma_N(t_0) \gg |\dot{\Gamma}_N/\Gamma_N|$, which implies $X_N \gg 1$ (for smoothly decaying rates). Thus there will be such integer $n_0 < N$ that

$$X_{n_0+1} > 1 > X_{n_0} \quad \text{and} \quad X_{n_0+1} \gg X_{n_0}. \qquad (9)$$

Under Eq. (7) it is sufficient to consider only three probabilities to be nonzero:

$$\{P_{n_0+1}, P_{n_0}, P_{n_0-1}\} = \{e^{-X_{n_0+1}}, e^{-X_{n_0}} - e^{-X_{n_0+1}}, 1 - e^{-X_{n_0}}\}. \qquad (10)$$

We see that the probability distribution is dominated by $P_{n_0} \to 1$ if $X_{n_0+1} \gg 1$ and $X_{n_0} \ll 1$. The meaning of this condition is simple: the state with $n_0 + 1$ electrons is unstable enough to have decayed while n_0 is stable.

Time-scale separation expressed by Eq. (7) can be taken into account directly in the most general solution (3), without requiring the same time dependence of $\Gamma_n(t)$'s. The mathematics of this derivation can be summarized as follows: observe that $\Gamma_{n+1}P_{n+1} = -\frac{d}{dt}\sum_{m>n}P_m$ exactly; assume that all $P_m(t)$'s with $m > n$ compared to $P_n(t)$ itself vary on a time scale much closer to t_0, so that $\Gamma_{n+1}(t')P_{n+1}(t') \propto \delta(t_0 - t')$ in Eq. (3); solve the resulting $P_n(\infty) = e^{-X_n}(1 - \sum_{m=n+1}^{N}P_m)$ to get

$$P_n(\infty) = e^{-X_n} \prod_{m=n+1}^{N} (1 - e^{-X_m}). \qquad (11)$$

Finally, examining Eq. (11) under condition (9) reveals a difference from Eq. (10) of at most X_{n_0}, which is reached at $X_{n_0} \ll X_{n_0+1} \approx 1$.

Parametric control of decay rate hierarchy.—The usefulness of Eq. (4) is limited unless the dependence of X_n's on commonly accessible external control parameters can be established. Typically, escape rates depend exponen-

tially on the height of the confining barrier, which in turn
can be controlled by a gate voltage V. Tuning the decay
rates $\Gamma_n(t)$ by V would affect all decay rates simultaneously. Thus we propose

$$\ln X_n = -\alpha_n V + \sum_{i=1}^{n} \delta_i. \quad (12)$$

Here, α_n and δ_n are phenomenological constants that can
be readily extracted experimentally as discussed below.

Figure 1(b) shows the behavior of the first two moments
for equal and fixed $\alpha_n = 1$ and $\delta_n = \delta$ ($\delta_1 = 0$ is a mere
shift of V). For $\delta > 6$ the difference between the approximations (4), (10), and (11) is negligible and Eq. (10) is
sufficient to describe the n_0th step of a staircase $\langle n \rangle(V)$
regardless of N. The minimal variance $\langle n - \langle n \rangle \rangle^2$ is
achieved at optimal values of V that are easily found
from Eqs. (10) and (12). The minimal value of $1 - P_1(V)$
decays roughly exponentially with δ.

Possible experimental realizations.—We expect to find
good candidates for experimental realization of the proposed initialization mechanism among dynamic-QD-based
electron pumps since backtunneling relaxation has been
found [10,14] to take place during certain parts of the pump
cycle. The pumped current I_{pump} consists of electrons
captured from the source and subsequently ejected into
the drain. It can be related to model prediction via

$$I_{\text{pump}} = ef\langle n \rangle \equiv ef\sum_n nP_n(\infty) \quad (13)$$

(f is the frequency which the pump cycle is repeated)
provided that (i) ejection to the drain starts after the escape
back to the source has stopped, and (ii) the ejection is
complete. In some experimental settings there is strong
evidence that the latter condition can be ensured [13,19]
while in others [10,11] conditions (i) and (ii) have been
conjectured based on electrostatic modeling.

We have used the ansatz (12) and the solution (4) in
Eq. (13) to fit experimental data from various electron
pump devices [15–17], the results are shown in Fig. 2. In
all cases α_n were found to vary weakly with n, so we have
set $\alpha_n = \alpha$ constant for the entire voltage range for each
device. Data set "a" in Fig. 2 was obtained in Ref. [15] for
a silicon nanowire metal-oxide-semiconductor field-effect
transistor (FET) driven by voltage pulses, while the data
labeled "b" correspond to a sinusoidal modulation of an
AlGaAs/GaAs nanowire metal-semiconductor FET in the
quantum Hall regime [16]. Yet another realization is exemplified by the data obtained in Ref. [17], for an
AlGaAs/GaAs split-gate device ("c" in Fig. 2), where
the time-dependent potential was generated by SAWs.
The voltage applied to the split gate superimposes the
SAW potential and tunes the height of the confining barriers corresponding to the control voltage V.

Figure 2 demonstrates the particular advantage of $\alpha_n = \alpha$: ($n - 1$)th step in $I_{\text{pump}}(V)$ has the length of δ_n on the
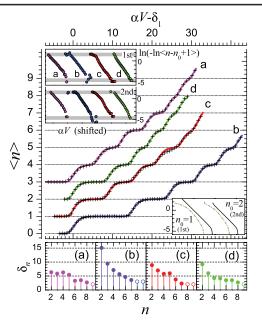scale of $\alpha V - \delta_1$. Thus, the set of voltage-independent

FIG. 2 (color online). Upper panel, main graph: decay-cascade
model fits (solid line) compared to measured current $I/(ef)$
(pluses) from Fig. 2a of Ref. [15] (a, magenta), Fig. 1a of
Ref. [16] (b, blue), and Fig. 1 of Ref. [17] (c, red), and to
classical simulation results from Fig. 6 of Ref. [11] (d, green).
The graphs are shifted vertically for clarity. Insets are discussed
in the text. Lower panels: fitted values of δ_n for each case.

$\delta_n = \ln X_n/X_{n-1}$ can be used as a fingerprint of a particular
device; see the lower panels in Fig. 2. Plotting $\ln(-\ln\langle n -
n_0 + 1\rangle)$ as a function of V serves as a quick test of the
ansatz (12) since the plateaux part dominated by X_{n_0} must
show up as a straight line. This is demonstrated in the lower
right inset of Fig. 2 for the analytic $\langle n \rangle$ with $\delta = 6$ [same
parameters as in Fig. 1(b)] and in the upper left inset for the
empirical data (same data sets as in the main panel). For
contrast, we show by a green dash-dotted line an *ad hoc* fit
with a sum of symmetric Fermi-like step functions; the
deviation from the cascade model is notable.

Our results for the second moment can be tested by
measuring the low-frequency shot noise power spectral
density [20]

$$S = 2e^2 f(\langle n^2 \rangle - \langle n \rangle^2). \quad (14)$$

Beyond the conditions (i) and (ii) discussed above, Eq. (14)
assumes [20] that (iii) the temporal width $d\tau$ of the electron
ejection current pulse is much less than the repetition
period, $d\tau f \ll 1$. This regime has been probed experimentally by Robinson and Talyanskii [21], and we find good
agreement with their data; see Fig. 3.

Discussion and outlook.—From the observations demonstrated in Figs. 2 and 3 we conclude that the decay-cascade initialization scheme can be readily implemented
experimentally. Several ways of controlling δ_n, thus
achieving more accurate initialization can be suggested:
(i) tighter confinement to increase the charging energy,
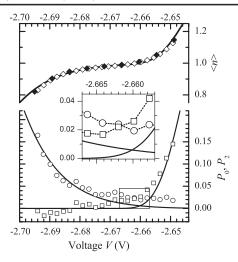(ii) employing more energy-selective barriers [22], or

FIG. 3.   Comparison to shot noise measurements on a SAW pump taken from Fig. 4a of Ref. [21]. Upper panel: measured $I_{pump}/(ef)$ [◆ from $I_{pump}(V)$, ◇ from $P_0(V)$ and $P_2(V)$] and calculated $\langle n \rangle$ (solid line). Parameters fitted in Eq. (4) with $N = 2$ and $\alpha_1 = \alpha_2$: $\alpha_1 = 92.04$ V^{-1}, $\delta_1 = -240.7$ and $\delta_2 = 6.252$. Lower panel and central inset: experimental probabilities P_0 (○) and P_2 (□) compared to Eq. (4) (solid line) with parameters derived from the fit to I_{pump}.

(iii) lowering the local temperature. Suggestion (iii) applies when escape is determined by thermal activation. Note that this classical regime was investigated in the electron dynamics simulations of Robinson and Barnes [11]; see trace "d" in Fig. 2, which demonstrates the universality of the decay-cascade model. Within a classical independent electron picture, δ_n would be controlled by the difference in barrier height for the most energetic electron, $\delta_n \approx a(E_n - E_{n-1})$ where E_n is the ionization energy of a QD with n electrons, and a is an inverse effective temperature in this picture. The experiment of Ref. [15] may have operated under these conditions since the reported temperature $T = 20$ K is relatively high. The value of $\delta_2 = 6.4$ from Fig. 2 then gives $E_C = 11$ meV in agreement the experimental estimate [15] $E_C = 10$ meV. In other implementations lowering the temperature of the device may be not that effective: comparing SAW- [17] and FET-based pumps [16] (traces c and b in Fig. 2 respectively), we see a large difference in δ_2 of the first plateaux. Despite a similarity in QD area, temperature and material implementation the maximally achievable accuracy according to our model is $\langle n - \langle n \rangle \rangle^2 \approx 10^{-3}$ for this particular SAW device versus 10^{-5} in the case of the FET. Assuming that tunneling dominates in the latter case, δ_n is expected to scale proportional to the difference in localization lengths between the ground states with n and $n - 1$ charges.

In conclusion, we have proposed a scheme for accurate initialization of QDs and analyzed it quantitatively. We have shown that the model may be readily implemented using nonadiabatic pump architectures. It allows us to extract a device-specific fingerprint which can be used to predict the results of a high precision measurement from a low precision characterization. In this way one can efficiently evaluate and optimize different pump architectures as required for fundamental metrology and adapt them for dynamic-QD-based quantum information devices.

Note added in proof.—After the final version of this Letter was submitted, single-electron quantum dot preparation with 15 ppm precision at $f = 340$ MHz in good agreement with the present model has been reported [23].

[1]   D. V. Averin and K. K. Likharev, *Mesoscopic Phenomena in Solids* (Elsevier, Amsterdam, 1991), p. 173.
[2]   D. Loss and D. P. DiVincenzo, Phys. Rev. A **57**, 120 (1998).
[3]   J. M. Elzerman *et al.*, Nature (London) **430**, 431 (2004).
[4]   C. H. W. Barnes, J. M. Shilton, and A. M. Robinson, Phys. Rev. B **62**, 8410 (2000).
[5]   G. Feve *et al.*, Science **316**, 1169 (2007).
[6]   M. Kataoka *et al.*, Phys. Rev. Lett. **98**, 046801 (2007).
[7]   T. Hayashi *et al.*, Phys. Rev. Lett. **91**, 226804 (2003).
[8]   C. Liu and Q. Niu, Phys. Rev. B **47**, 13031 (1993).
[9]   K. Flensberg, Q. Niu, and M. Pustilnik, Phys. Rev. B **60**, R16291 (1999).
[10] G. R. Aizin, G. Gumbs, and M. Pepper, Phys. Rev. B **58**, 10589 (1998).
[11] A. M. Robinson and C. H. W. Barnes, Phys. Rev. B **63**, 165418 (2001).
[12] M. D. Blumenthal *et al.*, Nature Phys. **3**, 343 (2007).
[13] S. Miyamoto *et al.*, Appl. Phys. Lett. **93**, 222103 (2008).
[14] C. Leicht *et al.*, Physica (Amsterdam) **42E**, 911 (2010).
[15] A. Fujiwara, K. Nishiguchi, and Y. Ono, Appl. Phys. Lett. **92**, 042102 (2008).
[16] B. Kaestner *et al.*, Appl. Phys. Lett. **94**, 012106 (2009).
[17] J. T. Janssen and A. Hartland, IEEE Trans. Instrum. Meas. **50**, 227 (2001).
[18] M. R. Astley *et al.*, Phys. Rev. Lett. **99**, 156802 (2007).
[19] B. Kaestner *et al.*, Appl. Phys. Lett. **92**, 192106 (2008).
[20] Y. M. Galperin, O. Entin-Wohlman, and Y. Levinson, Phys. Rev. B **63**, 153309 (2001).
[21] A. M. Robinson and V. I. Talyanskii, Phys. Rev. Lett. **95**, 247202 (2005).
[22] B. Kaestner *et al.*, Phys. Rev. B **77**, 153301 (2008).
[23] S. P. Giblin *et al.*, arXiv:1003.5862.